MULTIPLE SCLEROSIS JOURNAL | MSJ

Original Research Paper

Metabolic counterparts of sodium accumulation in multiple sclerosis: A whole brain ^{23}Na-MRI and fast ^{1}H-MRSI study

Maxime Donadieu, Yann Le Fur, Adil Maarouf, Soraya Gherib, Ben Ridley, Lauriane Pini, Stanislas Rapacchi, Sylviane Confort-Gouny, Maxime Guye, Lothar R Schad, Andrew A Maudsley, Jean Pelletier, Bertrand Audoin, Wafaa Zaaraoui and Jean-Philippe Ranjeva

Multiple Sclerosis Journal

2019, Vol. 25(1) 39–47

DOI: 10.1177/1352458517736146

Abstract

Background: Increase of brain total sodium concentrations (TSC) is present in multiple sclerosis (MS), but its pathological involvement has not been assessed yet.

Objective: To determine in vivo the metabolic counterpart of brain sodium accumulation.

Materials/methods: Whole brain ^{23}Na-MR imaging and 3D-^{1}H-EPSI data were collected in 21 relapsing-remitting multiple sclerosis (RRMS) patients and 20 volunteers. Metabolites and sodium levels were extracted from several regions of grey matter (GM), normal-appearing white matter (NAWM) and white matter (WM) T_2 lesions. Metabolic and ionic levels expressed as *Z*-scores have been averaged over the different compartments and used to explain sodium accumulations through stepwise regression models.

Results: MS patients showed significant ^{23}Na accumulations with lower choline and glutamate–glutamine (Glx) levels in GM; ^{23}Na accumulations with lower *N*-acetyl aspartate (NAA), Glx levels and higher Myo-Inositol (m-Ins) in NAWM; and higher ^{23}Na, m-Ins levels with lower NAA in WM T_2 lesions. Regression models showed associations of TSC increase with reduced NAA in GM, NAWM and T_2 lesions, as well as higher total-creatine, and smaller decrease of m-Ins in T_2 lesions. GM Glx levels were associated with clinical scores.

Conclusion: Increase of TSC in RRMS is mainly related to neuronal mitochondrial dysfunction while dysfunction of neuro-glial interactions within GM is linked to clinical scores.

Keywords: ^{23}Na-MRI, MRSI, multiple sclerosis, stepwise regression, neurodegeneration, demyelination

Date received: 9 May 2017; revised: 30 August 2017; accepted: 18 September 2017

Correspondence to:
M Donadieu
CRMBM Aix-Marseille University, CNRS, Faculté de Médecine, 27 Boulevard Jean Moulin F-13385, Marseille, France.
maxime.donadieu@etu.univ-amu.fr

Maxime Donadieu
Aix-Marseille University, CNRS, CRMBM, APHM, Marseille, France/Timone University Hospital, CEMEREM, Marseille, France/Siemens Healthineers, Saint-Denis, France

Yann Le Fur
Soraya Gherib
Ben Ridley
Lauriane Pini
Stanislas Rapacchi
Sylviane Confort-Gouny
Maxime Guye
Wafaa Zaaraoui
Jean-Philippe Ranjeva
Aix-Marseille University, CNRS, CRMBM, APHM, Marseille, France/Timone University Hospital, CEMEREM, Marseille, France

Adil Maarouf
Jean Pelletier
Bertrand Audoin
Aix-Marseille University, CNRS, CRMBM, APHM, Marseille, France/Timone University Hospital, CEMEREM, Marseille, France/APHM, Timone University Hospital, Department of Neurology, Marseille, France
CNRS, CRMBM UMR 7339, Medical School of Marseille, Aix-Marseille University, Marseille, France/AP-HM, CHU Timone, Department of Imaging, CEMEREM, Marseille, France/AP-HM, CHU Timone, Pole de Neurosciences Cliniques, Department of Neurology, Marseille, France

Lothar R Schad
Computer Assisted Clinical Medicine, Mannheim

Introduction

Multiple sclerosis (MS) is a multifocal autoimmune pathology of the central nervous system (CNS) affecting young adults, which is characterized by acute and chronic inflammation, demyelination and neurodegeneration.[1] Although neurodegeneration is considered to be the main substrate of irreversible disability in MS, this phenomenon is complex to characterize in vivo.[2] Mechanistic approaches have provided evidence that sodium accumulation is involved in neurodegenerative processes,[3,4] suggesting that measurement of in vivo brain sodium accumulation may be a relevant marker of neurodegeneration. Sodium (^{23}Na) MR imaging is a unique in vivo and non-invasive technique that enables quantification of total sodium concentrations (TSC) in the human brain.[5] Recently, clinical ^{23}Na-MRI studies have focused on MS, reporting abnormal increases of TSC in demyelinated white matter (WM) T_2 lesions, gadolinium-enhancing lesions,[6] normal-appearing white matter (NAWM) and grey matter (GM) of patients with different phenotypes of the disease including relapsing-remitting multiple sclerosis (RRMS)[7–9] and progressive multiple sclerosis (PMS) forms.[10,11] Nevertheless, as noted in a recent review, the meaning of observed brain sodium accumulations is unknown.[12] To refine information provided by ^{23}Na-MRI, the use of new MR contrasts have been proposed such as Triple Quantum Filtering (TQF)[13] and/or inversion recovery at high (3T) and ultra-high field (7T)[14] in

University Hospital, Heidelberg University, Mannheim, Germany

Andrew A Maudsley
Department of Radiology, University of Miami School of Medicine, Miami, FL, USA

order to separate sodium signals from the intra- and the extra-cellular compartments. Petracca et al.[13] used TQF to demonstrate decreases in intracellular volume fraction and increase in intracellular sodium concentrations in MS patients. However, these techniques not only suffer from very poor sensitivity requiring long acquisition times and leading to poor spatial resolution but also did not solve the interpretation of ^{23}Na-MRI.

Concurrently, complementary information on physiological and pathological processes can be obtained from metabolites detected using proton MR spectroscopic imaging, including (1) *N*-acetyl aspartate (NAA), which is synthesized in neuronal mitochondria[15] and considered to be highly linked to neuronal mitochondrial activity; (2) glutamate–glutamine (Glx), which provides a probe of neuro-astrocytic exchanges;[16] (3) total creatine (tCr), designating the signals of phosphocreatine and creatine, which is present in all cell types and considered to be an index of cellularity; (4) choline containing compounds (Cho), signals mainly detected in oligodendrocytes and astrocytes[17] and mostly associated with membrane (glycerophosphorylcholine), demyelination processes (free choline) and inflammation (Betaine); and (5) myo-inositol (m-Ins), a metabolite associated with glial cells, microglial activation and glial scar processes.[18]

The aim of this study was to better characterize the metabolic counterpart of total sodium accumulations within the different brain compartments (T_2 lesions, NAWM, GM) of RRMS patients in order to add specific cellular information to increase of TSC. To do so, we have examined the relationships between TSC derived from quantitative ^{23}Na-MRI and the corresponding metabolic maps of NAA, Glx, tCr, Cho and m-Ins assessed by volumetric proton echo planar spectroscopic imaging (3D ^{1}H-EPSI) optimized to sample the entire brain.[19]

Materials and methods

Subjects

This study was approved by the local Institutional Review Board (Marseille Provence 2) in accordance with the guidelines outlined in the Declaration of Helsinki. All subjects gave their written consent. For this exploratory study and according to previous studies providing significant results using similar techniques,[8,20] 21 RRMS patients (mean age = 37 ± 10.7 years, range = 23–59, 13 women, 8 men) and 20 healthy volunteers (mean age = 33.2 ± 10.2 years, range = 22–60, 12 women, 8 men) matched for age and sex ($p > 0.05$) were included in this study between February 2014 and July 2015.

^{1}H-MRI

MRI studies were performed on a 3-Tesla Magnetom Verio MR scanner (Siemens, Erlangen, Germany) using a 32-channel receiver head coil. The imaging protocol included sagittal T_1-weighted FLASH, axial 3D-T_1-weighted Magnetization Prepared RApid Gradient Echo (MPRAGE) (TE/TR/TI = 3.44/2150/1100 ms, voxel size = 1 × 1 × 1 mm^3, FOV = 256 mm, flip angle = 8°, matrix = 256^2, partitions = 176, acquisition time ≈ 5 minutes), axial T_2-weighted (TE_1/TE_2/TR = 11/90/8500 ms, FOV = 250 mm, flip angle = 150°, matrix = 256^2, thickness = 3 mm, 49 slices, acquisition time ≈ 4 minutes) sequences and sagittal fluid-attenuated inversion recovery (FLAIR) sequence (TE/TR/TI = 395/5000/1800 ms, voxel size = 1 × 1 × 1 mm^3, FOV = 250 mm, flip angle = 70°; matrix = 256^2, partitions = 160; acquisition time ≈ 6 minutes). Patients had also pre- and post-gadolinium injection T_1-weighted acquisitions to determine the presence of active lesions (TE/TR = 8.4/500 ms, FOV = 250 mm, flip angle = 70°, matrix = 256^2, thickness = 3 mm, 45 slices, acquisition time ≈ 4 minutes).

^{1}H-MRSI

Whole brain 3D-^{1}H-EPSI was acquired as described in Lecocq and colleagues,[19,20] using two axial acquisitions with two different orientations, one in the AC-PC plane and the other in the AC-PC + 15° plane (TE/TR/TI = 20/1710/198 ms, nominal voxel size = 1 × 1 × 1 cm^3, FOV = 280 × 280 × 180 mm^3, flip angle = 73°, 50 × 50 × 18 k-space points, GeneRalized Autocalibrating Partial Parallel Acquisition (GRAPPA) factor = 2, acquisition time ≈ 17 minutes) and the same 32-channel receiver head coil. Examples of spectra obtained across the brain are illustrated in Figure 1.

^{23}Na-MRI

^{23}Na-MR imaging was performed using a double tuned ^{23}Na-^{1}H volume head coil (Rapid Biomedical, Rimpar, Germany). The protocol, as described in Zaaraoui et al.,[8] included a density-adapted 3D radial projection reconstruction pulse sequence (TE/TR = 0.2/120 ms, 17,000 projections and 369 samples per projection, readout time per spoke = 20 ms, flip angle = 87°, nominal voxel size = 3.6 × 3.6 × 3.6 mm^3, acquisition time ≈ 34 min). External references (two tubes filled with 2% agarose doped with a sodium

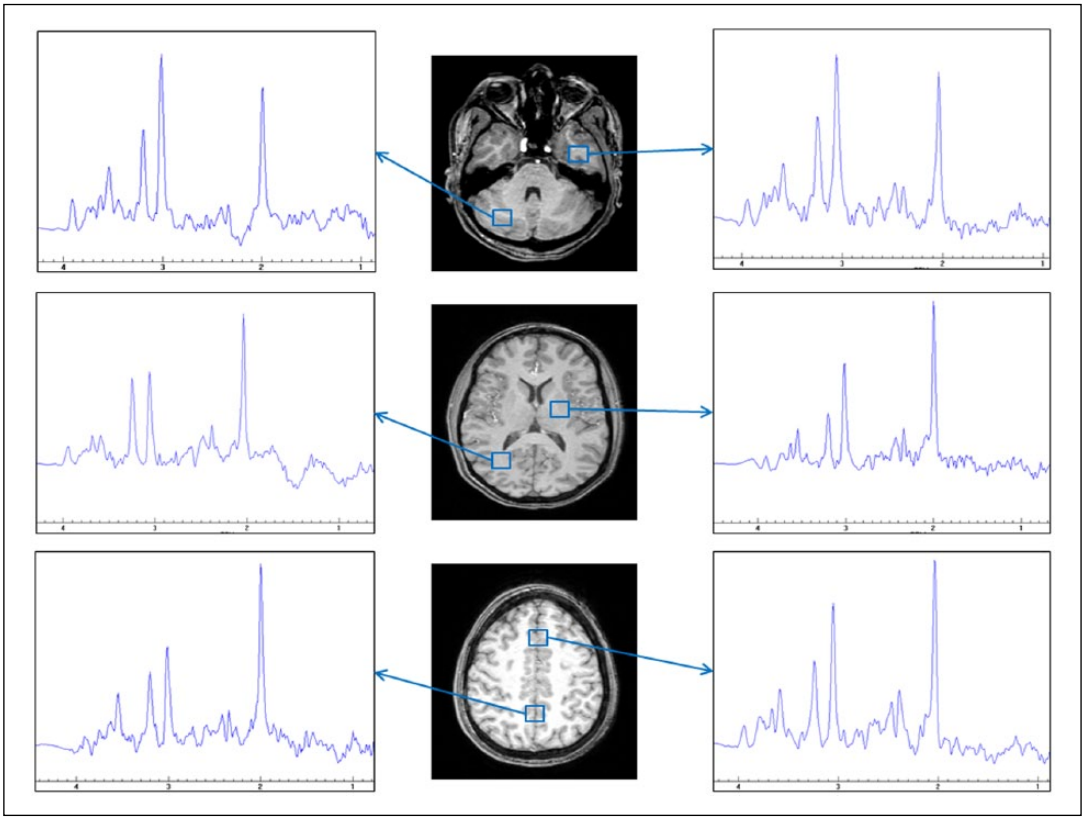

Figure 1. Examples of quality of spectra obtained over the whole brain using the 3D-^{1}H-EPSI sequence (male, 31 years old). The horizontal scale is shown in ppm.

concentration of 50 mmol/L) were placed on either side of the subject's head, in the field of view, for absolute sodium quantification.

The full acquisition time was approximately 1½ hours. After ^{23}Na-MRI acquisition performed with the double tuned ^{23}Na-^{1}H volume head coil, patient was repositioned in the scanner to perform the ^{1}H-MRI and ^{1}H-MRSI protocol using the 32-channel receiver ^{1}H head coil.

Data processing

Metabolic maps (Figure 2) obtained for each subject were post-processed and combined (AC-PC + AC-PC 15°) using the Metabolite Imaging and Data Analyses System (MIDAS, Trac, MRIR, Miami) software and SPM12 (Welcome Trust Centre for Neuroimaging at University College, London) following the procedure described in Donadieu et al.[20]

Radial ^{23}Na acquisitions were reconstructed via an in-house MATLAB (R 2011b, MathWorks Inc., Natick, MA) procedure.[21] Quantitative 3D ^{23}Na concentration maps (Figure 2) were obtained using the procedure described in Zaaraoui et al.[8] with SPM12.

WM T_2-lesion masks were delineated on T_2-weighted images by the same expert (S.G., with 4 years of experience) using a semi-automated method (interactive thresholding technique written on the Interactive Data Language platform, version 7.0; Exelis Visual Information Solutions, Inc.).[10]

All maps were spatially normalized in the same MNI space (SPM12). Segmentation of MPRAGE was performed using SPM12 and GM, WM, cerebrospinal fluid (CSF) density probability maps were spatially normalized in the MNI space.

For each patient, the transformation matrix obtained during the MNI spatial normalization of the T_2-weighted images was applied to its corresponding WM T_2 lesion mask to obtain the individual normalized WM T_2 lesion mask. Then, this mask was used as region of interest (ROI) to extract metabolic and ionic values from the normalized maps of the given patient and all controls. The procedure was redone for each patient to account for potential metabolic and ionic regional normal physiological variations in controls among the different spatial distributions matching the T_2 WM lesions in patients.

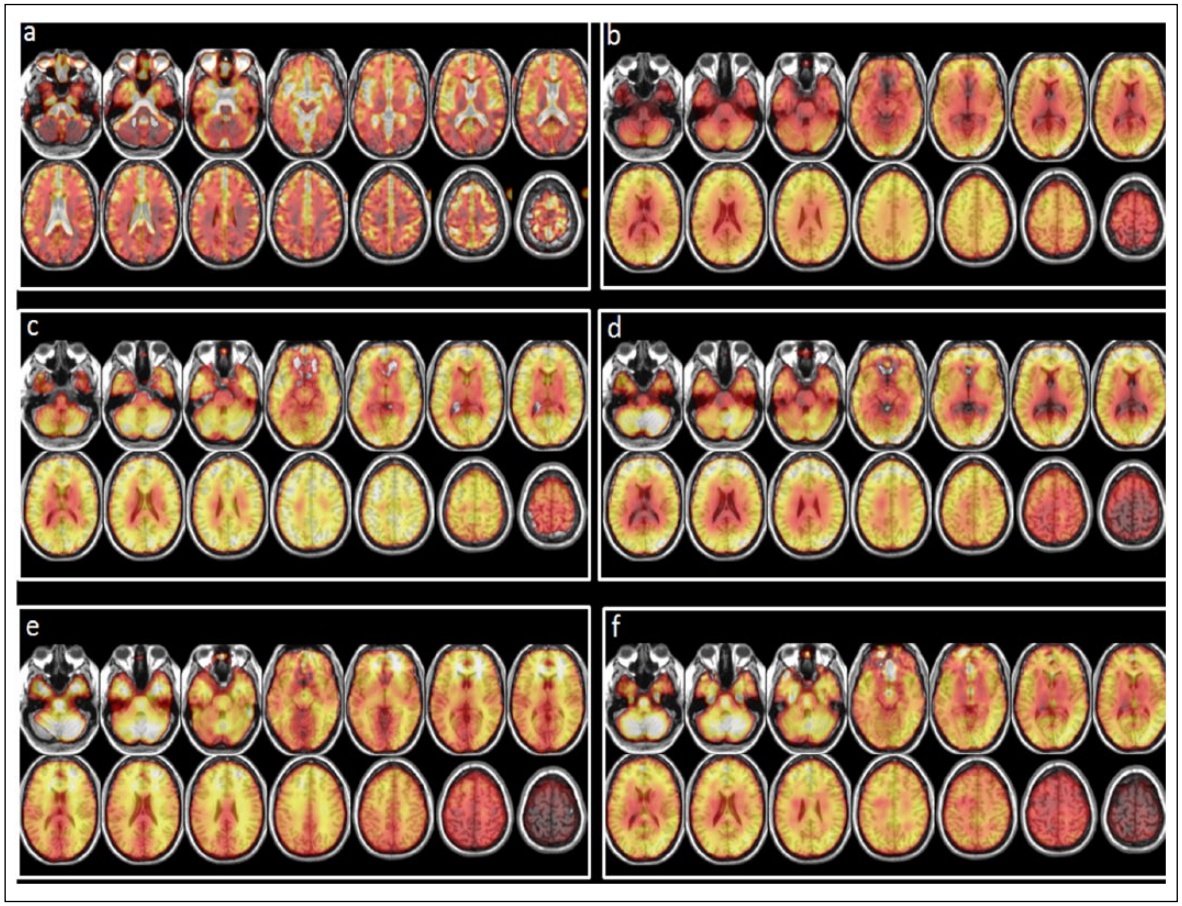

Figure 2. Examples of maps obtained from one subject (female, 29 years old) projected on MNI T_1 template: (a) sodium, (b) *N*-acetyl aspartate, (c) glutamate–glutamine, (d) total creatine, (e) choline and (f) myo-inositol.

To characterize metabolic and ionic profiles of MS patients within GM, spatially normalized ionic and metabolic maps were masked by the normalized GM probability density maps thresholded at 75% before extracting parameters from 90 GM ROIs (note that those including less than 20 voxels were not used) of the Automated Anatomical Labelling 2 (AAL 2) atlas.

To characterize metabolic and ionic profiles within the normal-appearing WM, all spatially normalized ionic and metabolic maps were masked by the normalized WM probability density maps thresholded at 75% (after subtraction of the normalized WM T_2 lesion masks) before extraction of parameters from the 12 WM regions corresponding to different lobes (frontal, parietal, limbic, temporal and occipital) (WFU pick atlas toolbox, SPM12).

These procedures were automated through a pipeline written in MATLAB (Figure 3). All ionic and metabolic values for each ROI were normalized using *Z*-scores based on the mean and standard deviation values obtained for the control group from the corresponding ROIs

$$\text{For each ROI: } Z\text{-score} = \frac{X - \mu}{\sigma}$$

where X = value of [^{23}Na], NAA, Cho, tCr, Glx, m-Ins for each subject; μ = mean value of [^{23}Na], NAA, Cho, tCr, Glx, m-Ins for the control group; and σ = standard deviation value of [^{23}Na], NAA, Cho, tCr, Glx, m-Ins for the control group.

For each parameter and each subject, the *Z*-scores were averaged across regions belonging to the same compartment to obtain *Z*-scores of GM, NAWM and WM T_2 lesions.

The *Z*-score allows us to calculate the standard deviation of a score compared to a control group and enables us to compare two scores that are from different normal distributions. *Z*-scores of ROIs belonging to each compartment (GM, NAWM) were averaged for

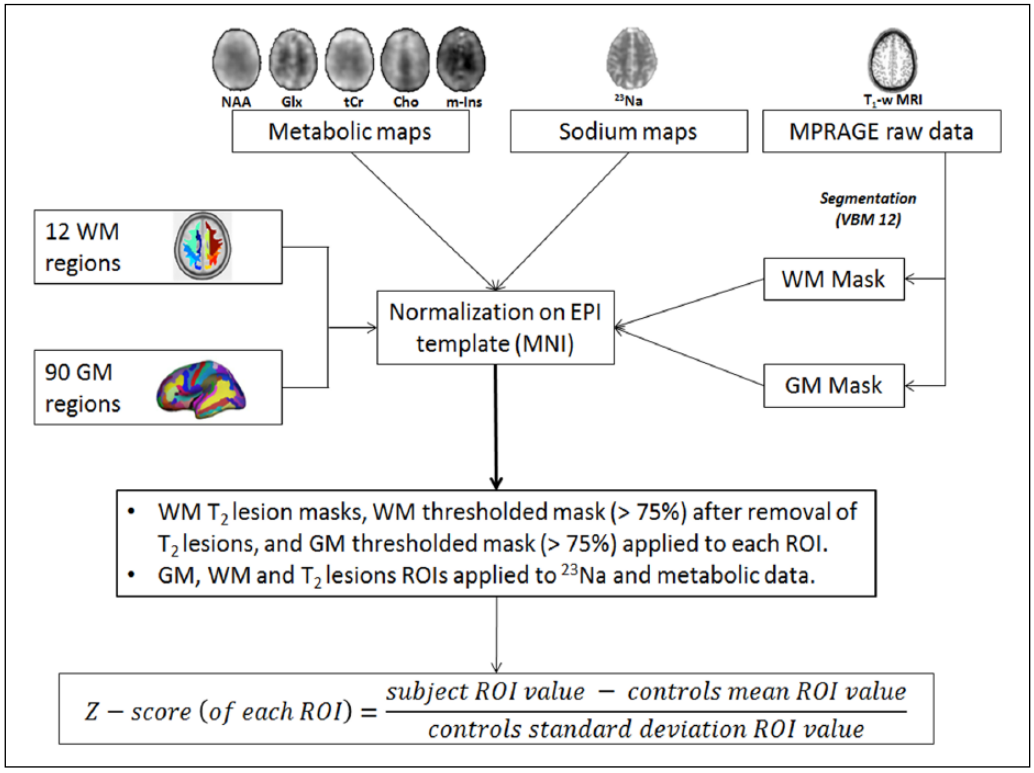

Figure 3. Post-processing pipeline including normalization in the MNI EPI spatial space, ^{23}Na and metabolites values extraction for each ROI of GM, WM and T_2 lesions and *Z*-scores computation.

each subject and each metabolic/ionic map. Note that for the computation of *Z*-scores corresponding to WM T_2 lesions, for each patient, control data values were obtained from ROIs defined as the individual spatially normalized WM T_2 lesion mask built for each patient and applied to the spatially normalized maps of all controls to extract mean and SD.

Clinical score assessment

Clinical status was assessed on the day of the MR examination using the Kurtzke Expanded Disability Status Scale (EDSS) and the Multiple Sclerosis Functional Composite (MSFC) score, which is composed of the paced auditory serial additional test (PASAT), the timed 25-foot walk (TFW) and the 9-hole peg test (9HPT).

Statistical analyses

Statistical analyses were performed with JMP 9 software (Version 13, September 2016, SAS institute). Wilcoxon rank tests were used to compare ionic and metabolic parameters observed between RRMS and controls within each independent compartment (GM, NAWM and WM T_2 lesions). The multiple comparison procedure considered the three compartments as independent leading to a Bonferroni correction factor of 6 ($p_{corr} < 0.008$).

To test the relationships between TSC and metabolite levels in RRMS patients, a stepwise regression model (forward) was performed for each compartment with $Z_{\text{-TSC}}$ as the dependent variable and $Z_{\text{-NAA}}$, $Z_{\text{-Glx}}$, $Z_{\text{-tCr}}$, $Z_{\text{-Cho}}$, $Z_{\text{-mIns}}$, GM%, WM% and CSF% as factors.

Correlations between average *Z*-scores ^{23}Na and *Z*-scores of metabolic parameters for each independent compartment were assessed using Spearman rank tests ($p < 0.05$, corrected by Bonferroni procedure with a Bonferroni factor of 5 $p_{corr} < 0.01$).

Finally, stepwise regression models (forward) were built to explain MSFC and EDSS with $Z_{\text{-NAA}}$, $Z_{\text{-Glx}}$, $Z_{\text{-tCr}}$, $Z_{\text{-Cho}}$, $Z_{\text{-mIns}}$, GM%, WM%, CSF% and T_2 lesion load as factors.

Results

On the day of the MR study, all patients were stable, exhibiting no gadolinium-enhancing lesions or relapses. In all, 81% of patients (17 out of 21) were

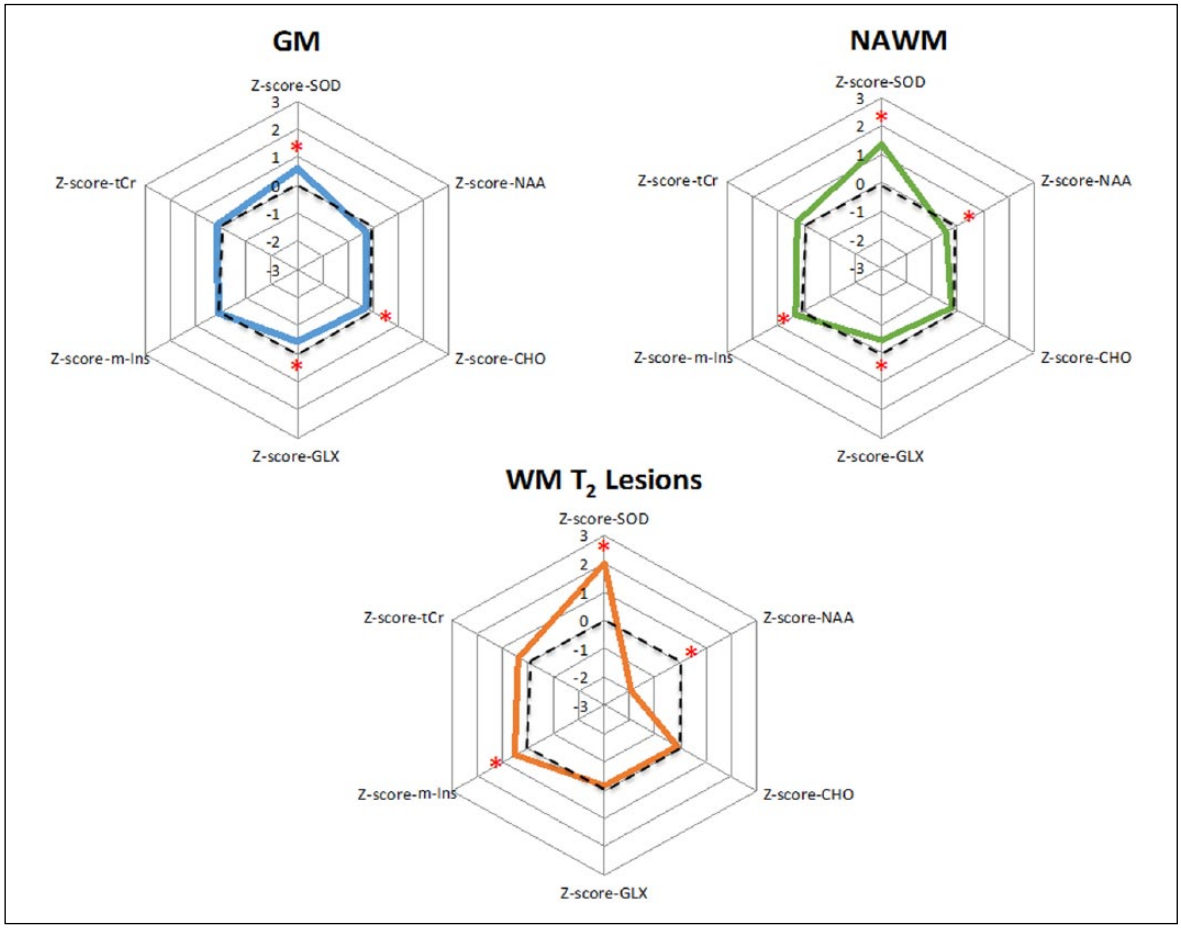

Figure 4. Radar plot of mean *Z*-scores of sodium and metabolites observed in RRMS patients within the three compartments (GM, NAWM, T_2 lesions). The asterisks indicate significant differences between patients and healthy controls (Wilcoxon test $p<0.05$ corrected by the Bonferroni procedure). Dotted lines represent the mean *Z*-scores of healthy controls (*Z*-score = 0).

under immunosuppressive or immunomodulatory disease-modified treatments. Median EDSS was 1, ranging from 0 to 4, median MSFC was −0.28, ranging from −5.82 to 1.58, and median disease duration was 5.6 years, ranging from 2.8 to 34.5 years.

Ionic and metabolic profiles of RRMS patients

All results are summarized in the radar plots shown in Figure 4. In GM, when compared to controls, RRMS patients showed significant increases in TSC ($p=0.0061$), with decreases in Cho ($p=0.0070$) and Glx ($p=0.0011$) and a trend of decreased NAA ($p=0.0610$) (Wilcoxon rank test).

In NAWM, RRMS had significant increases in TSC ($p=0.0002$) and m-Ins ($p=0.0053$), with decreases in NAA ($p=0.0232$) and Glx ($p=0.0167$).

Within T_2 WM lesions, RRMS showed significant increases in TSC ($p<0.0001$) and m-Ins ($p=0.0053$) and decreases in NAA ($p<0.0001$).

Association between total sodium accumulations and metabolite concentrations within the different brain compartments

Pairwise tests ($p<0.005$) show significant correlations between ^{23}Na *Z*-score and metabolites *Z*-score in the three compartments, especially between TSC and NAA. All the results are summarized in Supplemental Table 1.

For the GM compartment of RRMS patients, the stepwise regression model showed significant association between increases in TSC and decreases in NAA ($\beta=-0.831$; $p<0.0032$) (adjusted $R^2=0.341$, $p<0.0032$).

In NAWM, the stepwise regression model showed a significant association between increases in TSC and decreases in NAA ($\beta = -1.069$; $p < 0.0047$) (adjusted $R^2 = 0.346$, $p = 0.0085$).

Within WM T_2 lesions, increase in TSC was associated with decrease in NAA ($\beta = -1.261$; $p < 0.0001$) and smaller decrease in m-Ins ($\beta = -2.693$; $p = 0.0030$) and increase in tCr ($\beta = 2.822$; $p = 0.0017$) (adjusted $R^2 = 0.574$, $p = 0.0005$).

Correlation between clinical scores (EDSS, MSFC) and ionic or metabolic profiles

The stepwise regression model including all ionic and metabolic parameters and T_2 lesion load retained only the association between EDSS and decreased GM Glx ($\beta = -1.288$, $p = 0.0288$) (adjusted $R^2 = 0.187$, $p = 0.0288$).

Concurrently, MSFC was positively associated with GM Glx ($\beta = 1.066$, $p = 0.0123$) (adjusted $R^2 = 0.249$, $p = 0.0123$).

Discussion

We provide here, for the first time, the metabolic counterparts of total sodium accumulations observed in brain compartments of RRMS patients. A major challenge reached by this study is the assessment of whole brain ionic and metabolic samplings in vivo using ^{23}Na-MRI and fast 3D ^{1}H-EPSI acquisitions during the same clinical examination. In agreement with previous studies, we first confirmed the presence of abnormal cerebral increases of TSC in MS patients,[7,8,11] concomitant to decreased NAA within NAWM and T_2 WM lesions (trend for GM), decreased Glx within GM and NAWM, decreased Cho within GM, and increased m-Ins within NAWM and WM T_2 lesions.[20,22,23]

NAA decrease has been widely reported in RRMS patients within different brain regions including T_2 lesions,[24] NAWM,[24] deep GM[25] and cortical GM.[20] This decrease has been interpreted as both neuro-axonal damage and loss based on post-mortem histological studies.[18] The main result of this study was that the stepwise regression models accounting for tissue content mainly showed a negative correlation between total sodium accumulations and NAA levels. This is the first in vivo evidence that chronic brain increases of TSC are significantly related to mitochondrial neuronal dysfunction in all compartments. Previous in situ studies have proposed that sodium accumulations are related to neurodegenerative processes in MS.[3,4] Neuronal mitochondrial energy failure coupled with demyelination leads to Na^+/K^+ ATPase pump dysfunction and reorganization of sodium channels along axons.[4,26] Such dysfunction drives ^{23}Na accumulation inside the neurons and reverses Na^+/Ca^{2+} exchange activity. Ca^{2+} inflow stimulates a large array of Ca^{2+}-dependent enzymes like calpains, phospholipases or nitric oxide synthases, driving structural and functional axonal injury.[3,4]

While increase in glutamate has been observed in acute and active WM lesions reflecting excitotoxicity[27] and is considered a promising biomarker for MS disease progression,[28] the present decrease in Glx may reflect neuro-astrocytic metabolic dysfunctions within GM and NAWM.[16] Interestingly, the largest ionic/metabolic impact on global functional scores (EDSS and MSFC) was related to the GM Glx levels, in accordance with the fact that neuro-glial interactions occur preferentially in GM nearby synapses.[29] Whenever not surviving the stepwise regression model, paired correlations showed significant negative association between TSC and GM Glx levels, in line with the major role of sodium in neuro-glial interactions.[30] Study on experimental autoimmune encephalomyelitis (EAE) animal model highlights the major role of cytokines and glutamate on synaptic transmission deregulation and thereby on neurodegeneration, the main substrate of irreversible disabilities in MS.[31]

Decrease of Cho in GM appear to conflict with previous literature reporting increase of Cho in T_2 lesions,[32] NAWM and GM.[17] This apparent discrepancy with the majority of MRS works related to MS may be explained by the different metabolites included in the Cho peak having opposite behaviour during demyelination and demyelination-inflammation processes. Decreased Cho has been reported in inflammatory and non-inflammatory Cuprizone models of MS and interpreted as a decrease in glycerophosphatidylcholine (GPC).[33] Considering the whole group of patients relative to controls, the significant decrease of Cho levels could be interpreted as a large decrease of GPC reflecting mitochondrial dysfunction.[33] This lack of Cho increase can be linked to the random distribution of Cho increase undetectable in this group analysis or with decrease of GPC signal reflecting mitochondrial dysfunction.[33]

Increase of m-Ins in NAWM and T_2 lesions are also widely reported in the literature.[34] Indeed, m-Ins is involved in brain inflammation through glial activation (mostly astrocytes)[34] especially in the WM T_2 lesions during the early stages of MS (CIS, RR < 5

years),[22] spreading to NAWM after 5 years.[34] Increased m-Ins in NAWM and especially in WM T_2 lesions may reflect enhanced glial processes (scars and/or activation).

This exploratory study has some limitations. First, the sample size ($n=21$ patients) is relatively limited. Second, both imaging modalities suffer from relatively low signal to noise, which impacts spatial resolution and increases partial volume effects. We tried to minimize this effect by first applying WM and GM mask thresholds of 75% on ^{23}Na and ^{1}H-MRSI data. In addition to the masking procedure, we have included in the regression analyses the tissue content of ROIs characterized by WM%, GM%, CSF% and by removing ROIs composed by less than 20 voxels after masking. We proposed a clinically compatible MR protocol that provided acquisition of whole brain ^{23}Na-MRI and ^{1}H-MRSI, enabling metabolic and sodium brain concentrations to be measured within the same subjects in vivo and non-invasively. Even if the volumic images were easily spatially normalized in the common MNI template, these multimodal (multicontrast) images may suffer from registration errors that may impact the correlation measurements. Finally, even if metabolite maps were not expressed in absolute concentrations, metabolite signals were normalized by the interleaved water signal acquired during the same acquisition,[19] a procedure shown to be adequate even for multi-centre studies[35] but not accounting for potential changes in T_1 relaxation rates of water and metabolites.

In conclusion, a clinically compatible MR protocol was developed that provided acquisition of whole brain ^{23}Na-MRI and ^{1}H-MRSI, enabling metabolic and sodium brain concentrations to be measured within the same subjects in vivo and non-invasively. This study showed for the first time that the metabolic counterpart of total sodium accumulations observed in MS patients was related to neuronal mitochondrial dysfunction.

Future work will aim at deciphering the association between intracellular ^{23}Na concentrations and metabolic profiles using more specific methods of brain compartmentalization at ultra-high field (7T) such as TQF[13] or multi-TE sequences[14] allowing the separation of the contribution of restricted and free pools of sodium to the ^{23}Na-MRI signal.

Declaration of Conflicting Interests

The author(s) declared the following potential conflicts of interest with respect to the research, authorship and/or publication of this article: A.M., B.A. and J.P. received travel grants from commercial pharmaceutical companies: Biogen, Genzyme, Novartis, Merck Serono, MedDay, Roche and Teva. M.D., Y.L.F., S.G., B.R., L.P., S.R., S.C.-G., M.G., L.R.S., A.A.M., W.Z. and J.-P.R. have no relevant financial interest or relationship to disclose.

Funding

The author(s) disclosed receipt of the following financial support for the research, authorship and/or publication of this article: This study was supported by ARSEP Fondation, Association SEP Pays d'Aix, Agence Nationale de la Recherche (ANR-09-MNPS-025-SODIUMS, for the healthy control group). The first author is the recipient of a PhD Grant (CIFRE) supported by Siemens France and the French 'Association Nationale Recherche et Technologie' (ANRT).

References

1. Kutzelnigg A. Cortical demyelination and diffuse white matter injury in multiple sclerosis. *Brain* 2005; 128(11): 2705–2712.
2. Smith KJ. Sodium channels and multiple sclerosis: Roles in symptom production, damage and therapy. *Brain Pathol* 2007; 17(2): 230–242.
3. Freeman SA, Desmazières A, Fricker D, et al. Mechanisms of sodium channel clustering and its influence on axonal impulse conduction. *Cell Mol Life Sci* 2016; 73(4): 723–735.
4. Waxman SG. Axonal conduction and injury in multiple sclerosis: The role of sodium channels. *Nat Rev Neurosci* 2006; 7(12): 932–941.
5. Hilal SK, Maudsley AA, Ra JB, et al. In vivo NMR imaging of sodium-23 in the human head. *J Comput Assist Tomogr* 1985; 9(1): 1–7.
6. Eisele P, Konstandin S, Griebe M, et al. Heterogeneity of acute multiple sclerosis lesions on sodium (23Na) MRI. *Mult Scler* 2016; 22(8): 1040–1047.
7. Inglese M, Madelin G, Oesingmann N, et al. Brain tissue sodium concentration in multiple sclerosis: A sodium imaging study at 3 tesla. *Brain* 2010; 133(3): 847–857.
8. Zaaraoui W, Konstandin S, Audoin B, et al. Distribution of brain sodium accumulation correlates with disability in multiple sclerosis: A cross-sectional 23Na MR imaging study. *Radiology* 2012; 264(3): 859–867.
9. Maarouf A, Audoin B, Pariollaud F, et al. Increased total sodium concentration in gray matter better explains cognition than atrophy in MS. *Neurology* 2017; 88(3): 289–295.

10. Maarouf A, Audoin B, Konstandin S, et al. Topography of brain sodium accumulation in progressive multiple sclerosis. *Magn Reson Mater Phys Biol Med* 2013; 27(1): 53–62.

11. Paling D, Solanky BS, Riemer F, et al. Sodium accumulation is associated with disability and a progressive course in multiple sclerosis. *Brain* 2013; 136(7): 2305–2317.

12. Thulborn KR. Quantitative Sodium MR Imaging: A review of its evolving role in medicine. *Neuroimage* 2016; pii: S1053–8119(16)30674–30677.

13. Petracca M, Vancea RO, Fleysher L, et al. Brain intra- and extracellular sodium concentration in multiple sclerosis: A 7 T MRI study. *Brain* 2016; 139(3): 795–806.

14. Madelin G, Babb J, Xia D, et al. Repeatability of quantitative sodium magnetic resonance imaging for estimating pseudo-intracellular sodium concentration and pseudo-extracellular volume fraction in brain at 3 T. *Plos One* 2015; 10(3): e0118692.

15. Moffett JR, Ross B, Arun P, et al. N-Acetylaspartate in the CNS: From neurodiagnostics to neurobiology. *Prog Neurobiol* 2007; 81(2): 89–131.

16. Rae CD. A guide to the metabolic pathways and function of metabolites observed in human brain 1H magnetic resonance spectra. *Neurochem Res* 2014; 39(1): 1–36.

17. Kirov II, Tal A, Babb JS, et al. Serial proton MR spectroscopy of gray and white matter in relapsing-remitting MS. *Neurology* 2013; 80(1): 39–46.

18. Lassmann H. Mechanisms of white matter damage in multiple sclerosis. *Glia* 2014; 62(11): 1816–1830.

19. Lecocq A, Le Fur Y, Maudsley AA, et al. Whole-brain quantitative mapping of metabolites using short echo three-dimensional proton MRSI. *J Magn Reson Imaging* 2015; 42(2): 280–289.

20. Donadieu M, Le Fur Y, Lecocq A, et al. Metabolic voxel-based analysis of the complete human brain using fast 3D-MRSI: Proof of concept in multiple sclerosis. *J Magn Reson Imaging* 2016; 44(2): 411–419.

21. Nagel AM, Laun FB, Weber M-A, et al. Sodium MRI using a density-adapted 3D radial acquisition technique. *Magn Reson Med* 2009; 62(6): 1565–1573.

22. Fernando KTM, McLean MA, Chard DT, et al. Elevated white matter myo-inositol in clinically isolated syndromes suggestive of multiple sclerosis. *Brain* 2004; 127(6): 1361–1369.

23. Vingara LK, Yu HJ, Wagshul ME, et al. Metabolomic approach to human brain spectroscopy identifies associations between clinical features and the frontal lobe metabolome in multiple sclerosis. *Neuroimage* 2013; 82: 586–594.

24. Hattingen E, Magerkurth J, Pilatus U, et al. Combined 1H and 31P spectroscopy provides new insights into the pathobiochemistry of brain damage in multiple sclerosis. *NMR Biomed* 2011; 24(5): 536–546.

25. Geurts JJG, Reuling IEW, Vrenken H, et al. MR spectroscopic evidence for thalamic and hippocampal, but not cortical, damage in multiple sclerosis. *Magn Reson Med* 2006; 55(3): 478–483.

26. Witte ME, Mahad DJ, Lassmann H, et al. Mitochondrial dysfunction contributes to neurodegeneration in multiple sclerosis. *Trends Mol Med* 2014; 20(3): 179–187.

27. Srinivasan R. Evidence of elevated glutamate in multiple sclerosis using magnetic resonance spectroscopy at 3 T. *Brain* 2005; 128(5): 1016–1025.

28. MacMillan EL, Tam R, Zhao Y, et al. Progressive multiple sclerosis exhibits decreasing glutamate and glutamine over two years. *Mult Scler* 2016; 22(1): 112–116.

29. Kirischuk S, Héja L, Kardos J, et al. Astrocyte sodium signaling and the regulation of neurotransmission. *Glia* 2016; 64(10): 1655–1666.

30. Boscia F, Begum G, Pignataro G, et al. Glial Na(+) -dependent ion transporters in pathophysiological conditions. *Glia* 2016; 64(10): 1677–1697.

31. Centonze D, Muzio L, Rossi S, et al. The link between inflammation, synaptic transmission and neurodegeneration in multiple sclerosis. *Cell Death Differ* 2010; 17(7): 1083–1091.

32. Klauser AM, Wiebenga OT, Eijlers AJ, et al. Metabolites predict lesion formation and severity in relapsing-remitting multiple sclerosis. *Mult Scler* 2018; 24: 491–500.

33. Praet J, Orije J, Kara F, et al. Cuprizone-induced demyelination and demyelination-associated inflammation result in different proton magnetic resonance metabolite spectra. *NMR Biomed* 2015; 28(4): 505–513.

34. Fleischer V, Kolb R, Groppa S, et al. Metabolic patterns in chronic multiple sclerosis lesions and normal-appearing white matter: Intraindividual comparison by using 2D MR spectroscopic imaging. *Radiology* 2016; 281(2): 536–543.

35. Sabati M, Sheriff S, Gu M, et al. Multivendor implementation and comparison of volumetric whole-brain echo-planar MR spectroscopic imaging. *Magn Reson Med* 2015; 74(5): 1209–1220.